

## Do geochemical estimates of sediment focusing pass the sediment test in the equatorial Pacific?

Mitchell Lyle,<sup>1</sup> Neil Mitchell,<sup>2</sup> Nicklas Piasias,<sup>3</sup> Alan Mix,<sup>3</sup> Jose Ignacio Martinez,<sup>4</sup> and Adina Paytan<sup>5</sup>

Received 26 February 2004; revised 31 August 2004; accepted 25 October 2004; published 28 January 2005.

[1] The paleoceanographic recording fidelity of pelagic sediments is limited by chemical diagenesis and physical mixing (bioturbation and horizontal sediment transport). Diagenesis and bioturbation are relatively well-studied, but the effects of physical sedimentation have been largely ignored. Modeling U series isotopes (e.g.,  $^{230}\text{Th}$ ) can potentially quantify horizontal sediment movement, but model horizontal sediment focusing often equals or exceeds the vertical particle rain. We find no evidence of this level of sediment focusing in the equatorial Pacific from geophysical data or sediment core comparisons. The overestimate of sediment focusing by  $^{230}\text{Th}$  is probably caused by poor model assumptions: that sediment does not fractionate (does not sort according to size during transport) and that  $^{230}\text{Th}$  cannot leak from slowly accumulating sediments. Both assumptions are weak. U series methods do hold promise to quantify sediment focusing if properly calibrated. With calibration the trade-offs between seeking high sedimentation rates for better time resolution and the blurring by horizontal sediment focusing can be better assessed.

**Citation:** Lyle, M., N. Mitchell, N. Piasias, A. Mix, J. I. Martinez, and A. Paytan (2005), Do geochemical estimates of sediment focusing pass the sediment test in the equatorial Pacific?, *Paleoceanography*, 20, PA1005, doi:10.1029/2004PA001019.

### 1. Introduction

[2] Pelagic and hemipelagic sediments from the world's oceans are a fundamental archive of the evolution of earth conditions over the Cenozoic and late Mesozoic eras. The worth of this archive has long been recognized but it is also well known that pelagic sediments record conditions imperfectly. Much attention has been brought to bear upon the problems of diagenesis: the effects of chemical dissolution and slow equilibration between a nonequilibrium mixture of sedimentary components. Similarly, bioturbational mixing and its filter upon the preserved signal has been well-discussed. However, we know little about how sedimentation itself affects the paleoceanographic record, nor how changes in sedimentation may be recorded.

#### 1.1. U Series Estimates of Vertical and Horizontal Sediment Flux

[3] A series of papers have explored the use of U series isotopes to understand horizontal transport of sediments within the oceans and have highlighted this important problem [Higgins *et al.*, 1999; Marcantonio *et al.*, 2001; Chase *et al.*, 2003a; Loubere *et al.*, 2004; Francois *et al.*,

2004]. The U series method relies upon an essentially constant amount of uranium dissolved in ocean waters, coupled with decay to insoluble daughters (primarily  $^{230}\text{Th}$  but also  $^{231}\text{Pa}$ ). The daughter isotopes are rapidly sorbed to sedimenting particulate matter and fall to the bottom. Because the production rate of these daughter isotopes is well known, an estimate can be made of the horizontal component of sediment flux by comparing the daughter isotope flux accumulating in sediments with production in the immediately overlying water column [Francois *et al.*, 2004]. This methodology is attractive because a few simple measurements can be used to identify areas of large horizontal flux. Applications of these studies to data from the Antarctic has shown significant amounts of horizontal sediment transport [e.g., Chase *et al.*, 2003b] in a region where independent marine geological evidence has shown that large-scale horizontal sediment transport has occurred [e.g., Watkins and Kennett, 1971; Goodell *et al.*, 1971].

[4] Applying these same methods to the equatorial Pacific has identified another ocean region that appears to be strongly affected by horizontal sediment transport [Higgins *et al.*, 1999; Marcantonio *et al.*, 1996, 2001; Loubere *et al.*, 2004] but without independent evidence for horizontal sediment focusing. The estimates of sediment focusing in the equatorial western Pacific [Higgins *et al.*, 1999], central Pacific [Marcantonio *et al.*, 1996, 2001] and eastern Pacific [Loubere *et al.*, 2004] all suggest very high sediment focusing, up to or greater than the vertical particle flux falling from the productive surface waters overhead.

#### 1.2. Problems With High Sediment Focusing in the Equatorial Pacific

[5] Evidence independent of U series for high sediment focusing in the equatorial Pacific is lacking [e.g., Murray *et*

<sup>1</sup>Center for Geophysical Investigation of the Shallow Subsurface, Boise State University, Boise, Idaho, USA.

<sup>2</sup>School of Earth, Ocean and Planetary Sciences, Cardiff University, Cardiff, UK.

<sup>3</sup>College of Ocean and Atmospheric Sciences, Oregon State University, Corvallis, Oregon, USA.

<sup>4</sup>Departamento de Geología, Universidad EAFIT, Medellín, Colombia.

<sup>5</sup>Department of Geological and Environmental Sciences, Stanford University, Stanford, California, USA.

*al.*, 1993; Knappenberger, 2000; Thomas *et al.*, 2000; Murray *et al.*, 2000; Mitchell *et al.*, 2003]. Bulk sediment burial correlates with surface productivity, and so do a variety of indicators of paleoproductivity. Subsurface currents do not converge at the equator to focus the particulate matter, except at extremely shallow depths [Mantyla, 1975; Wyrki and Kilonsky, 1984; Bryden and Brady, 1985]. Shallow convergence of surface currents should not strongly affect the distribution of the particle-reactive Th and Pa because of the low residence time of particles in these layers and the high particle density. In other words, most of the  $^{230}\text{Th}$  produced by uranium decay in the shallow ocean should be removed by normal vertical particle flux.

[6] The geometry of postulated sediment focusing imposes important constraints not only on sedimentation but also on surface productivity and particle rain. If horizontal focusing of biogenic sediments to the equatorial region were high, the original particulate rain controlled by productivity must have been initially much more diffuse with latitude. Productivity should then not be particularly peaked at the equator, contrary to satellite estimates and surface measurements. Diffuse latitudinal distribution of productivity is also contrary to the latitudinal restriction in upwelled Fe from the Equatorial Undercurrent, a major factor in equatorial Pacific productivity and new production [Coale *et al.*, 1996; Chavez *et al.*, 1999; Le Bouteiller *et al.*, 2003].

[7] The horizontal focusing hypothesis should also cause a smooth distribution of sediment chemical properties since it implies diffusion and mixing of sediments over scales of  $10^2$  km or more. Horizontal focusing should erase sharp geographic changes in sediment composition (or paleoceanographic proxies) in the same way that bioturbation smooths a vertical compositional change. In the case of productivity-sensitive elements like Ba, one would expect to find latitudinal profiles to be poorly correlated with productivity and to find gradients in Ba to be more smooth than productivity. Neither of these predictions are realized. Barite accumulation rates in sediments are well-correlated with productivity along latitudinal profiles in the equatorial Pacific [Paytan *et al.*, 1996]. Profiles of sediment component ratios (e.g., Ba/Ti) are highly peaked at the equator [Murray *et al.*, 2000] indicative of weak horizontal transport at the large scales.

[8] The lack of independent evidence for sediment focusing via horizontal transport leads to two questions:

[9] 1. Are there alternate hypotheses that would require less sediment focusing but which are still consistent with U series systematics?

[10] 2. Can we test the level of sediment focusing independent of the U series data?

[11] On the basis of data we will discuss below, it is possible with core measurements and with subbottom seismic reflection profiling (both chirp and larger scale) to estimate sediment focusing independently. The sediment-based methods suggest that the  $^{230}\text{Th}$  method overestimates sediment focusing by as much as an order of magnitude. A serious disagreement between the  $^{230}\text{Th}$  model predictions and observations at the sea floor thus exists, which can be at least partly reconciled if the fine fraction of deep sea sediments travels independently of the coarse fraction. Such an expla-

nation would also explain the  $^3\text{He}$  results of Marcantonio *et al.* [1996] as Thomas *et al.* [2000] noted. Similarly, if  $^{230}\text{Th}$  and  $^{231}\text{Pa}$  leak out of the seafloor in areas of slow sedimentation (i.e., less than or equal to  $\sim 5$  mm/kyr, or more than half the Pacific Ocean) they should diffuse through the water column to regions of higher particulate rain. Either process causes a correlation between vertical particle rain and the burial of the U series isotopes and would exaggerate the apparent effect of sediment focusing at the equator.

## 2. Basics of Pelagic Sedimentation

[12] Pelagic sediments are unique because of slow mass accumulation rates (MAR) and the characteristic fashion that they drape over topography rather than filling basins first. Pelagic drape requires slow sedimentation and a low energy depositional regime at the seafloor so that particulate matter can be deposited almost independent of topography. An example of pelagic drape can be seen in Figure 1, a chirp subbottom profile (top) and a seismic reflection profile (bottom) along a survey line that passes across one core prominent in the sediment focusing controversy, Y69-71 [Loubere *et al.*, 2004; Lyle *et al.*, 2002a]). This north-south profile was taken during the NEMO-3 site survey for Ocean Drilling Program (ODP) Leg 202 and was used to choose the position of Site 1240, drilled at the position of ME005-24JC. Both the chirp and the seismic reflection profiles are typical of sediments found in the equatorial Pacific and in the Panama Basin where Y69-71 is located.

[13] Figure 1 shows the drape of the sediments over topography and the typical ability to trace seismic horizons for  $10\text{--}10^2$  km regionally. In the chirp profile of Figure 1 (top; 2–8 kHz Knudsen acoustic source) prominent seismic horizons mark ash layers from explosive volcanism in central America [Bowles *et al.*, 1973; Ninkovich and Shackleton, 1975; Drexler *et al.*, 1980]. Basement topography is covered with sediment from the top of the abyssal hills to the deepest basins despite the young age of the crust ( $\sim 2.5$  Ma; Mix *et al.* [2003]). Relatively high sediment deposition near the equator rapidly buries the faulted abyssal hills; sedimentation rates regionally are greater than 5 cm/kyr in the general vicinity of Y69-71 [Lyle, 1992]. The seismic reflection profile (bottom; 210 c.i. GI gun acoustic source) in Figure 1 shows that the sediments have deposited in this fashion essentially since sedimentation began, around 2.5 Ma. There has, however, been a consistent bias of sediment deposition to the deepest basin along the profile, where core ME005-24JC was taken.

[14] Tops of the abyssal hills collect only about 50% of the sediment flux compared to the ME005-24JC basin. The middle flat plain where Y69-71 was recovered collects sediment about 70% as fast as the ME005-24JC area. Because horizons can be easily traced throughout the profile and do not appear truncated, sediments probably bypassed the hills as they originally fell; they were not eroded and re-transported. Given the high current velocities needed for erosion compared to the typical  $<5$  cm/s abyssal currents, the lack of erosion is unsurprising [Lonsdale and Southard, 1974; Lister, 1976; Normark and Spiess, 1976; Lonsdale, 1977a].

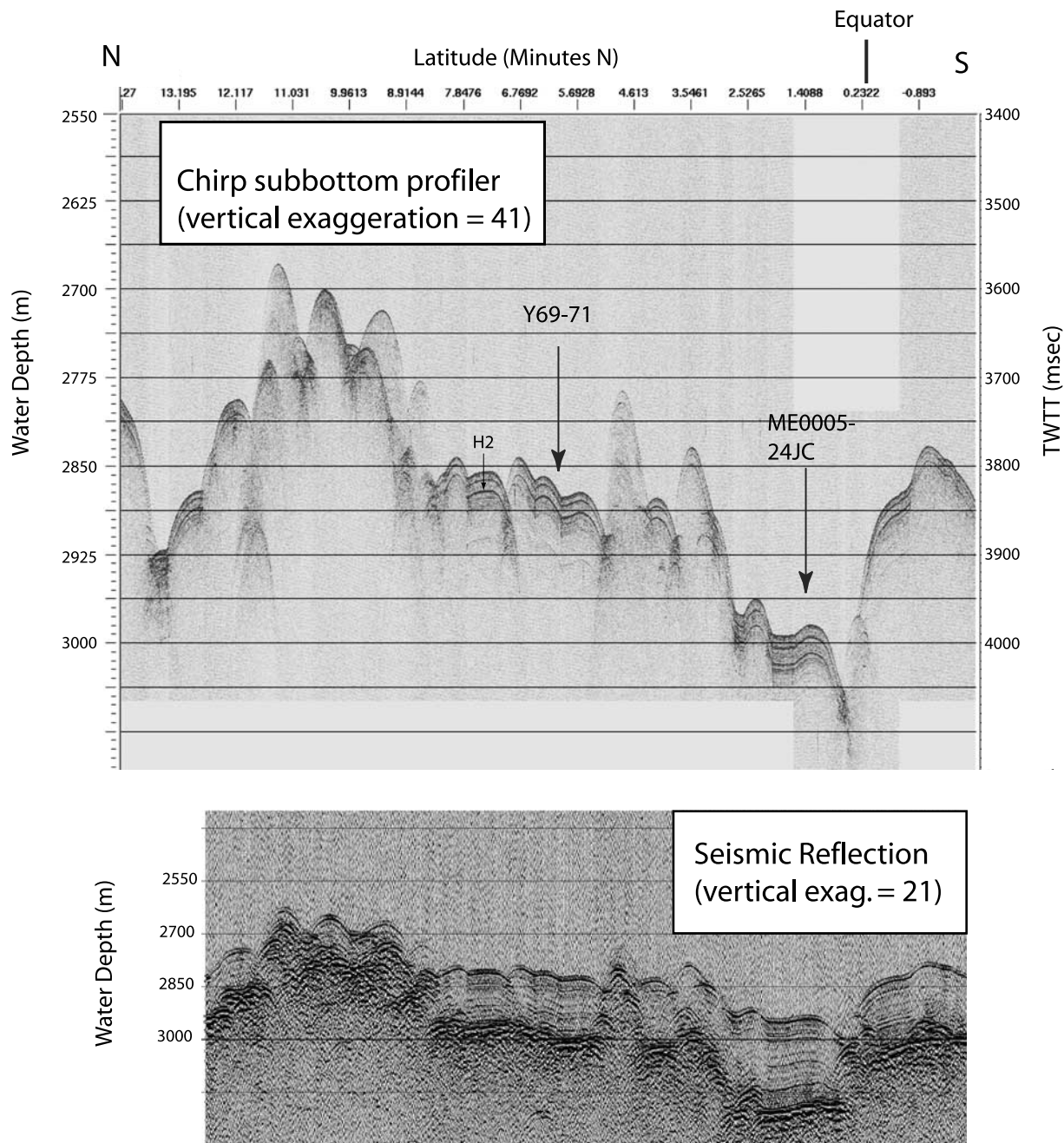


**Figure 1.** (top) High-resolution chirp subbottom profile and (bottom) GI-gun source seismic reflection profile along line 1 of the PAN-2 survey for ODP Leg 202. The survey passes across the site of core Y69-71, as discussed in the work of *Loubere et al.* [2004] and *Lyle et al.* [2002a] and ME0005-24JC (location of ODP Site1240). The entire area is sediment-covered, but tops of abyssal hills have about half the sediment thickness as the basin where ME0005-24JC is located. Sediment cover is not sufficiently variable locally to provide sufficient sediment for the level of sediment focusing estimated by  $^{230}\text{Th}$ .

[15] Do these differences in sedimentation matter, except in terms of the resolution of the records? If sediments are transported only small distances horizontally and if changes in sedimentation are coherent and of the same relative size to the mean long term sedimentation, these differences are of small importance. If sediments are transported large distances, thoroughly mixed, and the depositional changes

are random with respect to timing and geography, large errors could appear in a wide variety of paleoceanographic time series.

[16] There is a significant body of evidence that indicates pelagic sedimentation is coherent and in phase over large distances in pelagic realms. Good examples of the ability to correlate cores over long distances can be found by com-

paring between drill sites in the Initial Reports and Scientific Reports for ODP Legs 130, 138, 154, and 199, to name a few. Correlation of drill sites along the Leg 138 transect can be seen, for example, from well logs and physical properties profiles of the Leg 138 transect across the equatorial Pacific at 110°W [Lyle *et al.*, 1992; Harris *et al.*, 1995]. Such coherence suggests that horizontal sediment reorganization is not a major factor in deep sea sedimentation. Nevertheless, large-scale coherence of sedimentary deposition is not necessarily the case on continental slopes and basins, where we especially need to develop tools to study sediment focusing to validate high-resolution millennial-scale records. Similarly, there are events in the Cenozoic record of the equatorial Pacific that do occur and need to be studied in more detail [Mitchell and Lyle, 2005].

### 3. Extent of Horizontal Transport: The Focusing Problem

[17] It has been common to find  $^{230}\text{Th}$  records sometimes supported by  $^3\text{He}$  distributions that imply large horizontal transport and focusing of sediments in the equatorial Pacific region [Marcantonio *et al.*, 1996; Higgins *et al.*, 1999; Marcantonio *et al.*, 2001]. Paytan *et al.* [2004] address the implications of equatorial sediment focusing more thoroughly. We examine the implications of the magnitude of these fluxes, which are in the vicinity of a factor of 2 in the Holocene. A focusing factor of 2 implies that the horizontal sediment flux must be equivalent to the vertical flux. An area equivalent to the size of the depositional locale must be denuded of sediment to balance the sediment system, or a much larger area must lose part of its sediment cover.

[18] In the eastern equatorial Pacific a mass accumulation rate event during Last Glacial Maximum (LGM) that is also a major  $C_{\text{org}}$  burial event has been known for about 20 years [Pedersen, 1983; Lyle *et al.*, 1988; Pedersen *et al.*, 1991; Lyle *et al.*, 2002a]. Loubere and a variety of colleagues [Loubere, 1999; Loubere *et al.*, 2003, 2004; Francois *et al.*, 2004] have argued from benthic foraminiferal data that this was not a productivity event, and in the last two papers listed have used  $^{230}\text{Th}$  measurements to advance the case that horizontal transport and focusing actually produced the MAR spike. They estimate horizontal flux 8 times higher than the vertical flux during the peak of the MAR event in the LGM to account for the  $^{230}\text{Th}$  data. We will not divert ourselves speculating about why benthic foraminifera discriminate in their feeding against horizontally transported organic matter. Instead, we will explore whether there is any evidence from the sea floor that would corroborate the existence of a huge LGM horizontal sediment focusing event. Horizontal fluxes greater than a fraction of the vertical flux are easily measurable in cores and in geophysical profiles. If the horizontal flux is large, there should also exist large observable regions of abnormally thin or missing sediment from which the horizontal flux derived. There should be poor coherence between MAR records from cores inside and outside the focusing zone. We observe none of these patterns.

[19] The deep ocean, except near marine hydrothermal venting along the rise crest, produces negligible sediment.

Sediments in the deep sea are ultimately derived from the surface; they can only be redistributed or dissolved before they are buried. Away from continental margins and rise crests, the net accumulation summed over reasonably sized areas must be less than the vertical flux because diagenesis destroys significant fractions of biogenic particulate matter during burial and early diagenesis. Mass accumulation rates (MAR) measure the sum of production, diagenesis, and horizontal transport and must be used to close the system. Contrary to the opinion of Francois *et al.* [2004], MAR can be measured with sufficient accuracy to estimate fluxes on timescales of a few thousand years or less. Measuring bulk density is not difficult and can typically be done with an accuracy of a few percent.

[20] If sediments move horizontally, the movement will result in a region that has a net deficiency of sediment being buried and another region of excess. This will be observable by comparing MAR time series or by thickness of sediments between marker layers. If a horizontal flux estimate shows focusing of a factor of two, the sediment column should record that effect both in terms of thickness of sediments, observable by seismic reflection, or by MAR in individual core studies. It is possible to develop scales for horizontal transport, assuming a 4 km water column, as is average for the oceans. There is actually little information of typical deep current speeds outside of transects across the major deep flows, but the work that has been done shows that average current speeds are under 2 cm/s, and much of the currents are oscillatory, related to tides [Taft *et al.*, 1981; Fisher, 1984] so net transport is even smaller. Current speeds under NADW outflow [Schott *et al.*, 2004] might give a reasonable upper limit to steady deep current speeds. Schott *et al.* [2004] observe where NADW impinges on the abyssal bottom off the Grand Banks, the current speeds are less than 5 cm/s. Particulate matter falling through the water column has a vertical velocity greater than 100 m/day, based on the offset in time of flux spikes passing through the water column and laboratory experiments [Honjo, 1980, 1982]. Assuming a 4 km water column, 5 cm/s average current from surface to sea floor, and 100 m/day settling rate, a particle can travel only 170 km from its point of origin (or just over 1.5 degrees in latitude or longitude near the equator).

[21] Surface currents can be significantly faster than deep currents, but they have small vertical extent. For example, the South Equatorial Current can run as fast as 2 knots (100 cm/s), but its vertical extent is less than 200 m, so a particle traveling within the current travels less than a degree of longitude before falling out of its flow path. Immediately below is the equatorial undercurrent, which is of about the same vertical extent and flowing in the opposite direction. Net transport of particles should be small by these surface currents. The net surface and deep transport should be less than a degree (111 km).

#### 3.1. Panama Basin As a Test Site

[22] Geophysics provides tools to measure differences in sediment deposition since seismic horizons in equatorial Pacific seismic reflection profiles often mark time horizons [Mayer *et al.*, 1986]. In Panama Basin, the abundance of

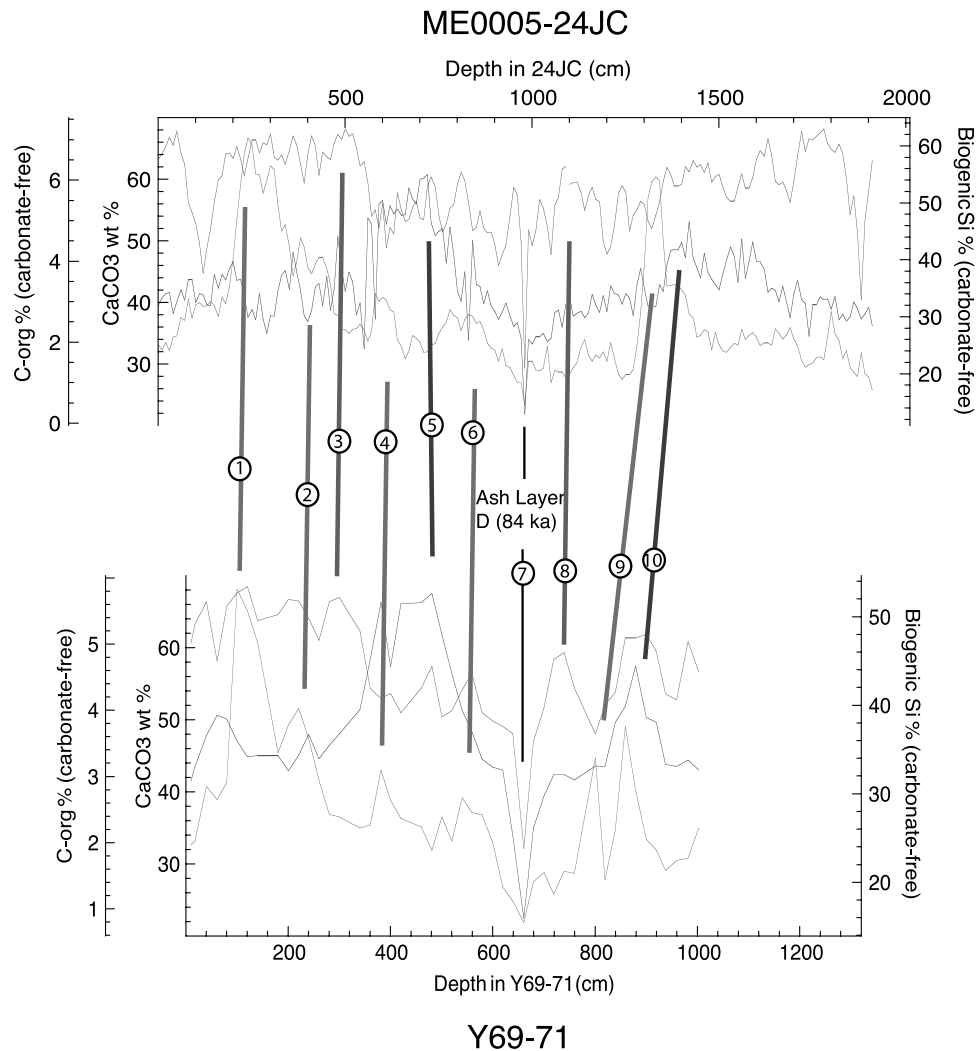


**Figure 2.** A comparison of  $\text{CaCO}_3$  (red), carbonate-free biogenic silica (purple), and carbonate-free  $\text{C}_{\text{org}}$  wt % (green) depth series between Y69-71 and ME0005-24JC. The cores have been lined up, and depths in each core are linearly scaled to each other based on ash layer D (84 ka; *Drexler et al.* [1980]). Lines mark correlations between the three records in each core, and numbers mark events in Figure 3. For at least the last 100 kyr, common sediment events between the two cores line up, indicating no change in relative sedimentation rate. See color version of this figure at back of this issue.

well-dated ash layers provides similar abilities in surficial sediments, which can be measured by chirp profiling. At a scale of 10–100 km we can use available seismic reflection data we have collected (some shown in Figure 1) to make an independent estimate of average sediment burial rates and focusing. We will use Y69-71 as an example core because it has a published  $^{230}\text{Th}$  sediment focusing estimate. *Louberé et al.* [2004] and *Francois et al.* [2004] estimate a Holocene focusing factor  $>2$  at Y69-71, rising to a factor of 8 at the LGM. In other words, *Louberé et al.* [2004] estimate that an amount of sediment equivalent to the vertical flux is now being supplied by horizontal sediment transport in the Holocene, while the LGM flux was absolutely dominated by horizontally transported sediments. By their estimate only 12% of the total LGM sediment column was supplied by vertical particulate rain. The rest came from somewhere else.

[23] Measurements on the chirp profile (top of Figure 1; from NEMO-3 (M. Lyle and N. Pisias, unpublished data, 2000)) can be used to make an independent estimate of horizontal sediment movement. We used the second major seismic horizon (H2, Figure 1, top), which is easily traceable throughout the area. This seismic horizon may represent ash layer “L” ( $\sim 230$  ka; *Ninkovich and Shackleton* [1975]) since its depth should be close to this age from local sedimentation rates. We have correlated the first subbottom seismic horizon (H1) to ash layer D (84 ka) at 9.8 m in ME0005-24JC. An ash at the appropriate depth for the second seismic reflector was found in Site 1240 (drilled at the location of 24JC) although it appears to be older than ash L [*Mix et al.*, 2003].

[24] Because the chirp profile was digitally acquired it can be manipulated to easily measure depth to seismic horizons.

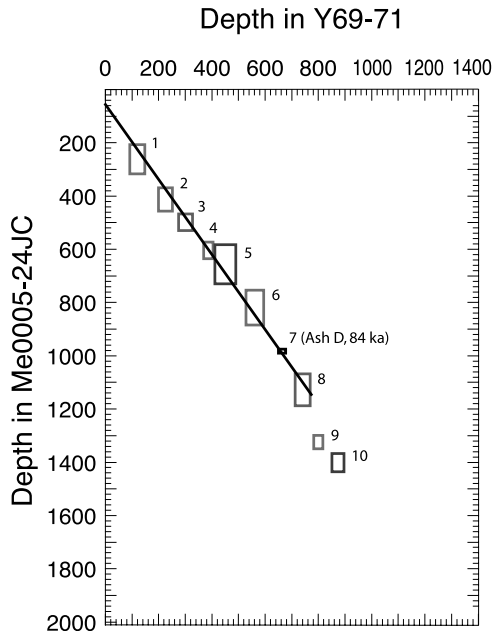


**Figure 3.** A Shaw plot to estimate relative sedimentation rates between Y69-71 and ME0005-24JC, showing that the relative sedimentation rate between the two cores has remained constant for the last 100 kyr. Each event shown in Figure 2 is represented by boxes here; red represents a  $\text{CaCO}_3$  event, purple represents biogenic silica, and green represents  $\text{C}_{\text{org}}$ . Numbers of the events are the same as in Figure 2. See color version of this figure at back of this issue.

Here we use a preliminary estimate but more thorough work is in progress. The mean thickness of sediments above H2 along the subbottom profile is 15.7 m using a sediment acoustic velocity of 1520 m/s. In the vicinity of Y69-71, we acoustically measure the depth to H2 to be 16.7 m, while in the ME0005-24JC basin the depth to H2 was estimated to be 23.6 m. The ash horizon at Site 1240 was found at 24.3 m [Miz et al., 2003]. The difference between the acoustically estimated versus the drilled depth illustrates the error associated with the velocity-depth conversion, about 3% of the total thickness. Because a constant acoustic velocity causes an error that increases with sediment thickness, there is a tendency to exaggerate depths in a thicker sediment piles and exaggerate sediment focusing in basins by this simple method.

[25] There is obvious sediment transport from the hills to the basins. Hills, which comprise about 51% of the profile, have an average sediment thickness of  $\sim 12.5$  m to H2, which balances the higher deposition elsewhere. In the vicinity of Y69-71 the depth to H2 was 16.7 m, or about 1 m greater than the 15.7 m average. Sediment focusing at Y69-71 thus should be less than 1.1 if supplied by local sediment redistribution, rather than the factor of 2 estimated by  $^{230}\text{Th}$ . The highest focusing factor along the profile, near core ME0005-24JC, is about 1.5, most of which comes from the highest abyssal hills. Clearly there is a major discrepancy between what we observe and what is estimated by  $^{230}\text{Th}$ .

[26] Depositional differences between the Y69-71 site and that of ME0005-24JC maintain themselves on all timescales, suggesting that the primary depositional process is time-invariant. One possible time invariant process is tidally induced sediment focusing or tidally induced internal waves [Cacchione et al., 2002]. Total sediment thickness to basement (i.e., for the last 2.5 Ma) exhibits a ratio of 1.45 for deposition at 24JC versus Y69-71. Taking a ratio of measurements to H2 in the chirp section gives a ratio of 1.41, while a comparison between common sediment events in the two cores consistently gives a ratio of 1.48 for the last 100 kyr.

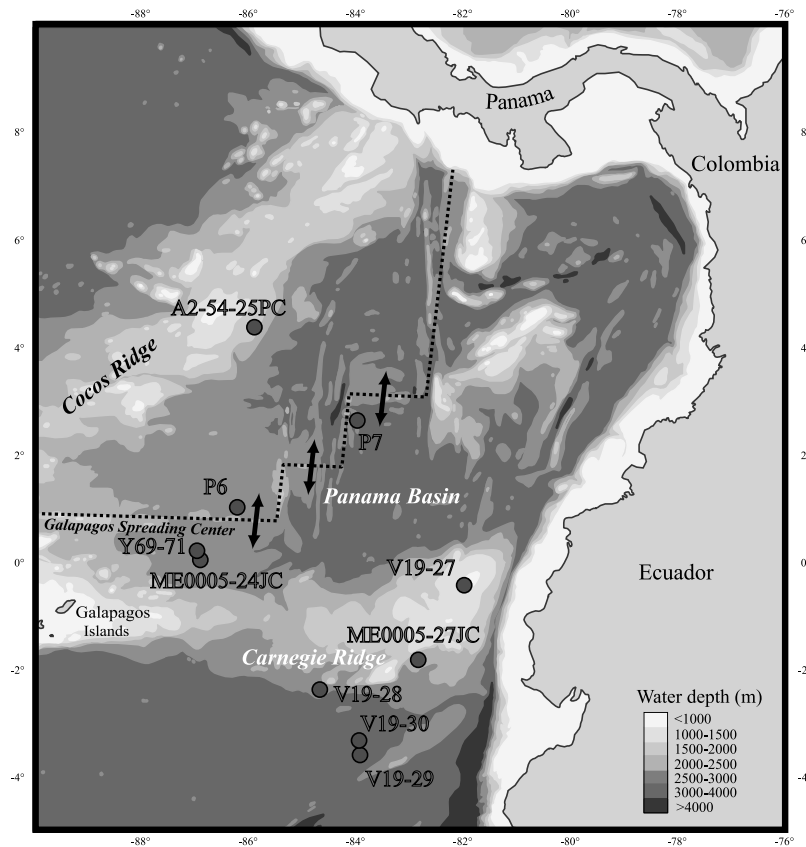
[27] Figure 2 shows a comparison between Y69-71 and ME0005-24JC using 3 separate biogenic records. The depths in the two cores have been linearly scaled in order that ash layer D [Drexler et al., 1980] lines up between the two cores. Figure 3 is a Shaw plot of the depth of each event in one core versus the other. We use carbonate-free biogenic Si and  $\text{C}_{\text{org}}$  records to remove any dilution effects from the biogenic time series that might introduce spurious coherence between the records. It is clear that both cores have similar time series even though the average sedimentation rate in ME0005-24JC is nearly 1.5 times higher than Y69-71. For about the last 100 kyr we observe essentially the same relative sedimentation rates between cores, so a MAR record from one core is coherent with one from the other, and either MAR record should have the same paleoceanographic information. We also observe that Y69-71 is missing the uppermost part of the sediment column, with the topmost sediment of Y69-71 being equivalent to 50 cm in ME0005-24JC, or about 5 ka. Occasionally there is significant stretching or squeezing needed to match the core records (e.g., between 700 and 900 cm in Y69-71) which would indicate differential sedimentation between them, or a coring artifact. Nevertheless, a MAR record from either core could easily be used to predict the other. The local redistribution (“sediment focusing”) that does occur is extremely constant over very large time frames and relatively large distances.

[28] Sediment burial measured on timescales from millions of years to thousands of years indicate a time-independent horizontal transport from the higher ground around Y69-71 to the basin where ME0005-24JC was recovered. The basin provides an expanded record, but we do not observe incoherent sedimentation events between records indicative of large-scale variability. The cause of the LGM MAR spike is at a greater horizontal scale than that of the abyssal hill topography, i.e., greater than tens of km.

### 3.2. Other Cores and the Panama and Peru Basins

[29] We can also easily correlate the biogenic records from these two cores, for example, to V19-28, 300 km to the southeast, and to ME0005-27JC, more than 400 km to the east (Figure 4). Such scales are about a factor of 3 larger than the upper limit for scales of horizontal sediment transport, as we discussed earlier. Large-scale geographic coherence implies a primary control by the vertical particulate rain.

[30] The Last Glacial Maximum MAR spike is found not only in deep topography of the Panama and Peru Basins ( $>2.5$  km) but also in a small basin on top of the Carnegie Ridge (core V19-27, 1373 m). Sediment focusing should preferentially fill basins but if anything should cause ero-



Scale: 1:9375375 at Latitude 0°

**Figure 4.** A map of the Panama Basin and northern Peru Basin showing where the Last Glacial Maximum sedimentation event has been found [Lyle *et al.*, 2002a; Pedersen *et al.*, 1988; Lyle *et al.*, 1988; Pedersen, 1983; M. Lyle and J. Guarin-Tirado, unpublished data, 2001]. This event is not confined to a small area. Instead, it has been found over a 6° square of the Panama Basin and northern Peru Basin east of the Galapagos. If this event were to be caused by sediment focusing, much of the rest of the eastern tropical Pacific must have been stripped of sediment during the Last Glacial Maximum. There is insufficient area on ridges to provide sediment for focusing. See color version of this figure at back of this issue.

sion on the high topography. Finding the event in less than 1500 m of water severely limits the source region for sediment. If the source is re-suspended sediment, there is insufficient high topography around the Panama Basin to produce a sediment focusing event. Occam's razor suggests that a change in the vertical particulate rain is the best explanation for the LGM spike.

[31] Loubere *et al.* [2004] note that the MAR at V19-27, on top of the Carnegie Ridge, is half that of Y69-71, in the Panama Basin. However they did not explain why both records are coherent and why they both have the same magnitude LGM CaCO<sub>3</sub> MAR spike, relative to their mean MAR [Lyle *et al.*, 2002a]. They argued for local sediment processes fortuitously producing similar effects at both cores. Again, the simplest explanation is a common sedimentation event, from surface waters.

[32] There is no evidence in the seismic reflection data around Y69-71 and ME0005-24JC for sufficient sediment focusing at a local scale to validate the <sup>230</sup>Th estimate. Nor

do we find any evidence for a regional erosion event to supply sediment for focusing. Lyle *et al.* [2002a] have identified regionally coherent patterns of CaCO<sub>3</sub> MAR and identified the scale of a LGM event. The regional extent of cores which have the LGM sediment MAR spike (Figure 4) indicates that the event is widespread and not likely to be a result of focusing. The area where the MAR spike has been found occupies a region greater than 6° by 6°. If a factor of 8 increase in deposition occurred at the Last Glacial Maximum to cause this event sediment should be entirely missing from a nearby 17° square to balance the system. We are capable of finding an anomaly of this scale fairly easily but do not observe it.

[33] Finally, let us assume that the <sup>230</sup>Th measurements at Y69-71 of Loubere *et al.* [2004] actually represent sediment focusing and look at the paleoceanographic implications. The only realistic source region for excess sediment in this region of the Panama Basin is the Galapagos Platform, where the eastward flowing Equatorial Undercurrent breaks

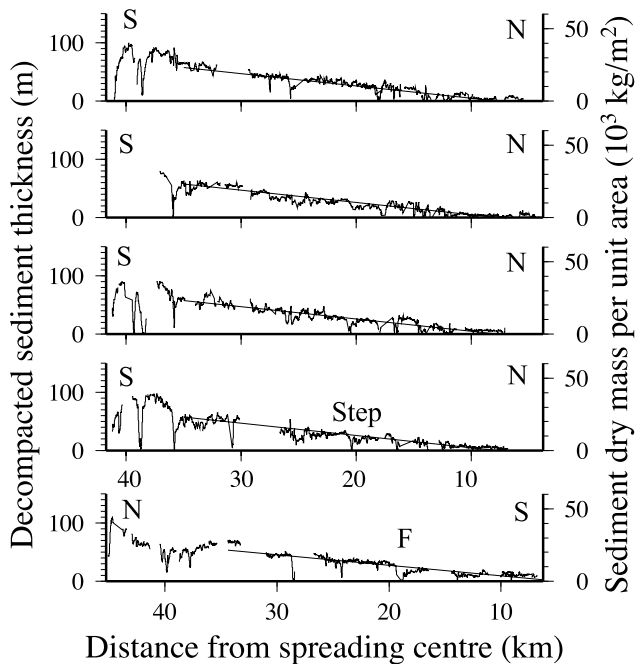


**Figure 5.** Measurements of sediment thickness derived from sediment profiler records collected along five transects perpendicular to the Galapagos Spreading Center (four from the south flank and one from the north flank) at about  $86^{\circ}\text{W}$ . See Figure 3 for the spreading center location. The data are corrected for compaction using DSDP physical property data and are presented as the equivalent dry sediment mass per unit sea floor area [Mitchell, 1998]. The straight lines are least squares regressions of thickness against distance. The data show remarkably systematic trends with a short-length-scale fluctuation due to locally varied deposition on the rough volcanic topography and erosional scour around fault scarps (such as where marked by “F”). Sediment thickness in places abruptly increases across fault scarps, such as where marked by “Step,” reflecting the pattern of near-axis lava flows [Mitchell, 1995].

up [Pak and Zaneveld, 1973], and which could provide significant sediment. The Galapagos Platform has roughly the same area as the Panama Basin region bounded by the Galapagos Spreading Center to the north and the Carnegie Ridge to the south, the region that we know to have coherent sedimentation. It is barely possible, if essentially all the Holocene sediment were removed from the platform to the area surrounding Y69-71, to match the Holocene focusing factor estimated by  $^{230}\text{Th}$ . However, 4 times as much sediment would have to come from the region at the LGM to match the  $^{230}\text{Th}$  estimate of LGM sediment focusing, requiring an enormous productivity event confined to the Galapagos platform to produce the sediment. This makes no paleoceanographic sense.

### 3.3. Other Studies in the Panama Basin

[34] Other large data sets can also be exploited to study sediment focusing in the Panama Basin (Figure 5) [Klitgord and Mudie, 1974; Lonsdale, 1977b; Mitchell, 1995, 1998].

High-resolution sediment profiler records were collected around the Galapagos Spreading Centre with the Scripps Deep Tow system in the 1970s [Klitgord and Mudie, 1974; Lonsdale, 1977b], about 50 km north of the Y69-71 core location (Figure 4). Sediment thicknesses derived from these data vary in a systematic way around the spreading center [Mitchell, 1995, 1998], with no evidence for the large-magnitude variations of deposition rates to be expected from the U series results.

[35] Figure 5, derived from five long profiles taken roughly perpendicular to the spreading center, shows a general systematic thickening of the sediment pile with distance. These trends are consistent with a simple progressive buildup of the sediment cover over time, because the underlying basement systematically ages with distance as a result of seafloor spreading. The average MAR inferred from these data are equal on the two sides of the ridge [Mitchell, 1998]. Superimposed on these trends is a short-length-scale fluctuation due to sediments filling the fine-scale relief of the lava surface, digitizing precision, and erosion around fault scarps [Klitgord and Mudie, 1974; Mitchell, 1996]. The data reveal some further details, such as step changes in sediment thickness across fault scarps. These are most likely caused by the different ages of ridge axis lava flows which are bounded by the escarpments [van Andel and Ballard, 1979], leaving a stepped pattern in basement age and hence thickness of accumulated sediment [Mitchell, 1995]. To quantify these observations, we derived the data variogram  $\gamma_h$  by first dividing the data by the regression lines in Figure 5 and then calculating the following from the resulting normalized data  $s_i$  for distances greater than 10 km from the spreading center:

$$\gamma_h = \sum_{i=1}^{n-h} \frac{(s_i - s_{i+h})^2}{2n}, \quad (1)$$

where  $h$  is the lag and  $n$  are the number of overlapping data contributing to the variogram (i.e., allowing for gaps in the data series). Figure 6 shows these variograms (gray lines) along with an average variogram (continuous dark line) and an exponential model fitted to the average (dotted curve). The short-length-scale fluctuation in the data cause the variogram to rise up to 1 km lag (the fitted exponential has an e-folding length of only 300 m) before reaching a sill with  $\gamma_h = 0.09$ . This sill value is a measure of the data variance and implies that sediment thicknesses vary with a standard deviation of only 0.3 times the mean value (i.e., the uncorrelated fluctuation is only 30% of the mean). The small anomaly in Figure 6 for lags between 1 and 4 km is due to intermediate-scale variability probably associated with the lava flows. We see no evidence for the large-magnitude nonsystematic fluctuations in deposition that have been claimed from the U series data.

### 3.4. Other Studies in the Equatorial Pacific

[36] We also have a seismic profile from the vicinity of the JGOFS equatorial Pacific experiment to MANOP Site C ( $\sim 1^{\circ}\text{N}$ ) [Knappenberger, 2000; Mitchell et al., 2003], which Marcantonio et al. [2001] have suggested might be a source region for equatorially focused sediment. Profiles of the sediment thickness can be found in the work of Mitchell et

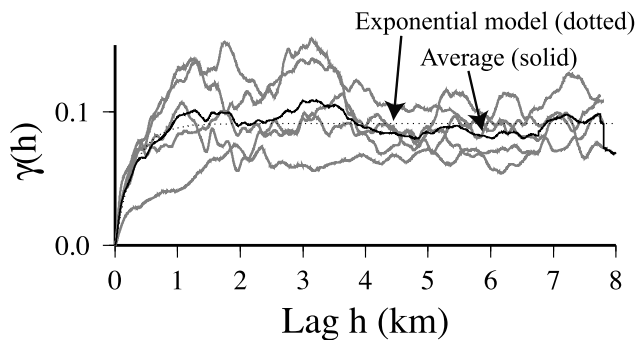


**Figure 6.** Variograms (gray lines) computed from the data in Figure 4 after normalizing to remove the systematic trends. The dark continuous line is the average of the variograms, and the dotted line is a simple exponential model fitted to it (see text). The rise in the variogram before  $h = 1$  km represents the short-wavelength variability. The sill (variogram tendency with increasingly large  $h$ ) represents the data variance ( $A = s^2$ ), which here suggests that the uncorrelated fluctuations have a standard deviation  $s$  of only 0.3 times (30% of) the mean value.

*al.* [2003]. The U series estimate of the focusing factor averages about a factor of 2 at the equator. We observe a change in thickness above the 4.2 Ma Green reflector from 43 m at the equator to 31 m at Site C. The sedimentologically derived maximum focusing factor is thus  $\sim 1.2$ , assuming constant primary production and particulate rain from the equator to  $1^\circ\text{N}$ . Sediment trap fluxes measured along a similar transect dropped by 30% between the equator and  $2^\circ\text{N}$  [Honjo *et al.*, 1995]. Essentially all of the observed change in sediment thickness can thus be accounted for by changes in particulate rain associated with distance from the equatorial upwelling maximum.

#### 4. Why Does Sediment Focusing Fail the Sediment Test?

[37] The  $^{230}\text{Th}$  method fails because it is based upon an oversimplified model of Th sedimentation. The Th sedimentation model is actually a constant authigenic sedimentation model similar to one used to estimate growth rates of manganese nodules via their Co content [e.g., Somayajulu *et al.*, 1971]. It is less robust, however, because the  $^{230}\text{Th}$  model adds another weak assumption, that the initial flux of  $^{230}\text{Th}$  can be globally predicted and need not be measured [Francois *et al.*, 2004]. Since an individual  $^{230}\text{Th}$  measurement will always be internally consistent with the model, errors can only be estimated through external comparisons. Our measurements suggest the errors to be very high, perhaps as much as a factor of 10.

[38] We suggest that the major errors in the  $^{230}\text{Th}$  method occur because the model expects “perfect” sedimentation [Francois *et al.*, 2004], i.e., (1) that the particulate rain is assumed to be a single component that does not fractionate, and (2) that  $^{230}\text{Th}$  is removed from the ocean system as soon as the sediment reaches the seafloor. Both of these assumptions cause overestimates of sediment focusing in regions of

high particle flux, and overestimate loss of sediment from low sedimentation regimes.

#### 4.1. Preferential Movement of $^{230}\text{Th}$ in a Fine Particulate Fraction

[39] The distribution coefficient of  $^{230}\text{Th}$  is  $10^6$  to  $10^7$  [Chase *et al.*, 2002]. Once  $^{230}\text{Th}$  is produced in the water column it is rapidly adsorbed onto the particulate fraction. Because adsorption is a function of surface area,  $^{230}\text{Th}$  will be preferentially adsorbed to the small, high surface area particles such as clays, and will be affected by the same sedimentation processes that sort fine and coarse sediment particles as they fall through the sediment column. Within the water column and at the benthic boundary layer, there is an opportunity for a strong net horizontal flux of  $^{230}\text{Th}$  without significant bulk sediment movement.

[40] The fine particle fraction of suspended sediments is also preferentially swept out of the water column by high sedimentation, for example under regions of high productivity which produce large amounts of marine “snow.” There should be a correlation between particle flux and  $^{230}\text{Th}$  flux. If the vertical particle flux is insufficient to sweep the  $^{230}\text{Th}$  production to the sea floor, a net transport of fine particles (and  $^{230}\text{Th}$ ) should ensue from regions of low particle rain to regions of high particle rain. In the “perfect sedimentation” model, this diffusion is modeled as horizontal sediment focusing although it could represent essentially zero actual flux. Such particle diffusion would explain correlations between  $^3\text{He}$  and  $^{230}\text{Th}$  [Marcantonio *et al.*, 1996, 2001] without large levels of bulk sediment focusing. The diffusion of the fine fraction has been explored extensively by Thomas *et al.* [2000], who argue that  $^{230}\text{Th}$  in excess of production should be a measure of particle flux and paleoproductivity.

[41] A dependence of  $^{230}\text{Th}$  flux on particle flux has actually been observed in sediment trap experiments [e.g., Bacon *et al.*, 1985; Chase *et al.*, 2003b]. If there were an independent estimate of the magnitude of particulate rain we could correct the  $^{230}\text{Th}$  measurements for the variation in particulate rain. However, the dependence between  $^{230}\text{Th}$  flux and bulk flux in sediment traps has been used to indicate variable trap efficiency [Yu *et al.*, 2001a, 2001b] rather than variable Th scavenging efficiency or fine particle fractionation correlated to vertical flux. In other words, undertrapping of Th and other U series isotopes in the water column is assumed to indicate that an equivalent vertical flux was lost in the trapping process.

[42] The assumption that  $^{230}\text{Th}$  is unfractionated in the particulate rain is thus built into the “trapping correction.” Because of this underlying assumption, variations in  $^{230}\text{Th}$  fractionation are interpreted to be an artifact of the trapping process rather than a fundamental observation. “Corrected” sediment trap fluxes are not as correlated, unsurprisingly, to the  $^{230}\text{Th}$  flux. Nevertheless, even the corrected data still have a strong correlation between the magnitude of vertical flux and capture of  $^{230}\text{Th}$  [Yu *et al.*, 2001b].

#### 4.2. Leakage of $^{230}\text{Th}$ From Slowly Accumulating Sediments

[43] It is well known [e.g., Bacon and Anderson, 1982] that the Th isotope distribution between suspended particulate

ulate matter and seawater shows Th to be readily and reversibly exchanged. The exchange between seawater and particulate matter falling through the water column profoundly affects distributions of all the U series elements. Adsorption-desorption processes also occur in the surface sediments, which can then leak back into the overlying water column. In areas of extremely slow sedimentation, such diffusion out of the sediments might be a significant fraction of the total  $^{230}\text{Th}$  deposited.

[44] Essentially all the Pacific gyres (latitudes between  $5^\circ$  to  $45^\circ$ ) are regions of extremely low sedimentation rates, mostly averaging below 5 mm/kyr. In the coring associated with ODP Leg 199 site surveys, for example, we were able to core to sediments as old as middle Eocene ( $\sim 45$  Ma) with 15–20 m piston cores [Lyle *et al.*, 2002b]. Rates of sedimentation of the piston-coreable surface sediments between  $6^\circ\text{N}$  and  $20^\circ\text{N}$  thus ranged from around  $2\text{ mm}/10^3\text{ yr}$  to  $0.3\text{ mm}/10^3\text{ yr}$ , or an order of magnitude lower than rates typically thought to be slow pelagic sedimentation rates.

[45] In the Pacific gyres, almost none of the particulate rain is preserved and the adsorbed  $^{230}\text{Th}$  released at the sea floor by particle dissolution is a large potential source of leakage back to the ocean. The few comparisons between sediments and sediment traps indicates that in these low sedimentation rate (“red clay”) environments more than 95% of the original particulate flux is dissolved at the sea floor (e.g., Dymond and Lyle [1994]; 96% at MANOP Site H and 99% at MANOP Site S). The  $^{230}\text{Th}$  carried by particles dissolved at the benthic boundary layer must reorganize onto other surfaces or diffuse back to the ocean.

[46] It is possible to examine manganese nodules to test whether a diffusive loss of  $^{230}\text{Th}$  is plausible. The Manganese Nodule Project, for example, studied one nodule from the central Pacific at about  $11^\circ\text{N}$  [Moore *et al.*, 1981] and found strong evidence for  $^{230}\text{Th}$  mobility. They noted that both the top and the bottom of the nodules were simultaneously growing and incorporating unsupported  $^{230}\text{Th}$ , indicating that excess  $^{230}\text{Th}$  was able to diffuse at least 3 cm into the sediment. The excess  $^{230}\text{Th}$  inventory on the bottom or buried side of the nodule was 5% of the top exposed to seawater. In addition, the inventory of the top side of the nodule was only 2/3 that expected from production in the overlying water column, again indicative of significant diffusive leakage. Large areas of the Pacific sea floor adjacent to the equatorial region can thus be a significant source of  $^{230}\text{Th}$  that could be transported to the equatorial Pacific to be stripped by the high particulate flux.

## 5. A Lack of Data

[47] There is a frustrating lack of data to study the problem of horizontal sediment transport and calibrate the

$^{230}\text{Th}$  system. For example, bathymetric data at the JGOFS equatorial Pacific sediment trap moorings were never collected, nor were a sufficient quantity of cores taken to resolve the sediment focusing issue. We have no other sediment trap deployments to constrain the problem in better surveyed parts of the equatorial Pacific. The only equatorial sediment trap deployment in the eastern Pacific, between  $80^\circ$  and  $140^\circ\text{W}$ , was early in the development of sediment traps and did not trap quantitatively [Cobler and Dymond, 1980]. We have no measure of equatorial particulate fluxes to calibrate eastern Pacific studies. We have never really designed a geophysical survey and coring program to adequately resolve the issue of sediment redistribution, nor have we adequately studied water-column particulates and their horizontal displacement to quantitatively estimate horizontal sediment movement. Relatively modest field programs could take care of these deficiencies, however.

## 6. Conclusions

[48] The use of the  $^{230}\text{Th}$  method to estimate sediment focusing has a beguiling appeal of simplicity but unfortunately does not appear to produce a correct estimate of the magnitude of horizontal sediment transport and focusing. The method is not yet properly calibrated for use as a sediment focusing indicator. Several of the assumptions used to keep the  $^{230}\text{Th}$  model simple render conclusions based upon  $^{230}\text{Th}$  alone dubious. Where it is possible to actually compare model results to sediments we have found that  $^{230}\text{Th}$  strongly overestimates sediment focusing. In the Panama Basin sediment focusing estimated from seismic profiles is significantly smaller than the vertical flux of particulate rain, on the order of 10–50% of the average sedimentation rate in the region surrounding the core Y69-71. Estimates of sediment focusing by  $^{230}\text{Th}$  are 100–800% of the vertical particulate flux, in contrast. Simple analyses we have presented show that potential source areas are much too small to provide the sediment and current speeds are insufficient to concentrate such a significant amount of sediment.

[49] Small-scale sediment focusing does exist, and can cause thickened sections in basins. However, we have observed sedimentary records typically to be regionally coherent, so that one record can be linearly scaled to another. The coherent sedimentation regions tend to match surface water patterns and do not correlate with bathymetric features, contrary to predictions from sediment focusing.

[50] **Acknowledgments.** We thank the crew and technical support staff of the R/V *Melville* for their help in gathering the site survey data shown here. Financial support of this work was covered by NSF grants OCE-9907292 (ACM, NP, and MWL) and OCE-0240906 (MWL). NCM gratefully acknowledges receipt of a University Research Fellowship from the Royal Society, which supported his contribution to this work.

## References

- Bacon, M. P., and R. F. Anderson (1982), Distribution of thorium isotopes between dissolved and particulate forms in the deep sea, *J. Geophys. Res.*, *87*, 2045–2056.
- Bacon, M. P., C.-A. Huh, A. P. Fleer, and W. G. Deuser (1985), Seasonality in the flux of natural radionuclides and plutonium in the deep Sargasso Sea, *Deep Sea Res.*, *32*, 273–286.
- Bowles, F. A., R. N. Jack, and I. S. E. Carmichael (1973), Investigation of deep-sea volcanic ash layers from equatorial Pacific cores, *Geol. Soc. Am. Bull.*, *84*, 2371–2388.

- Bryden, H. L., and E. C. Brady (1985), Diagnostic model of the three-dimensional circulation in the upper equatorial Pacific ocean, *J. Phys. Oceanogr.*, *15*, 1255–1273.
- Cacchione, D. A., L. F. Pratson, and A. S. Ogston (2002), The shaping of continental slopes by internal tides, *Science*, *296*, 724–727.
- Chase, Z., R. F. Anderson, M. Fleisher, and P. Kubik (2002), The influence of particle composition and particle flux on scavenging of Th, Pa, and Be in the ocean, *Earth Planet. Sci. Lett.*, *204*, 215–229.
- Chase, Z., R. F. Anderson, M. Fleisher, and P. Kubik (2003a), Accumulation of biogenic and lithogenic material in the Pacific sector of the Southern Ocean during the past 40,000 years, *Deep Sea Res.*, *50*, 799–832.
- Chase, Z., R. F. Anderson, M. Fleisher, and P. Kubik (2003b), Scavenging of  $^{230}\text{Th}$ ,  $^{231}\text{Pa}$ , and  $^{10}\text{Be}$  in the Southern Ocean (SW Pacific sector): The importance of particle flux, particle composition and advection, *Deep Sea Res.*, *50*, 739–768.
- Chavez, F., P. G. Strutton, G. Friederich, R. A. Feely, G. C. Feldman, D. G. Foley, and M. J. McPhaden (1999), Biological and chemical response of the equatorial Pacific Ocean to the 1997–1998 El Niño, *Science*, *286*, 2126–2131.
- Coale, K. H., S. E. Fitzwater, R. M. Gordon, K. S. Johnson, and R. T. Barber (1996), Control of community growth and export production by upwelled iron in the equatorial Pacific ocean, *Nature*, *379*, 621–624.
- Cobler, R., and J. Dymond (1980), Sediment trap experiment on the Galapagos Spreading Center, equatorial Pacific, *Science*, *209*, 801–803.
- Drexler, J. W., W. I. Rose Jr., R. S. J. Sparks, and M. T. Ledbetter (1980), The Los Chocoyos Ash, Guatemala: A major stratigraphic marker in middle America and in three ocean basins, *Quat. Res.*, *13*, 327–345.
- Dymond, J., and M. Lyle (1994), Particle fluxes in the ocean and implications for sources and preservation of ocean sediments, in *Material Fluxes on the Surface of the Earth*, edited by W. W. Hay et al., pp. 125–143, Natl. Acad., Washington, D. C.
- Fisher, K. (1984), Particle fluxes in the eastern tropical Pacific Ocean—Sources and processes, Ph.D. dissertation, Oreg. St. Univ., Corvallis.
- Francois, R., M. Frank, M. M. Rutgers van der Loeff, and M. P. Bacon (2004),  $^{230}\text{Th}$  normalization: An essential tool for interpreting sedimentary fluxes during the late Quaternary, *Paleoceanography*, *19*, PA1018, doi:10.1029/2003PA000939.
- Goodell, H. G., M. A. Meylan, and B. Grant (1971), Ferromanganese deposits of the South Pacific Ocean, Drake Passage, and Scotia Sea, in *Antarctic Oceanology I*, *Antarct. Res. Ser.*, vol. 15, edited by J. L. Reid, pp. 27–92, AGU, Washington, D. C.
- Harris, S., T. K. Hagelberg, N. G. Pisias, and N. J. Shackleton (1995), Sediment depths determined by comparisons of GRAPE and logging density data during Leg 138, *Proc. Ocean Drill. Program Sci. Results*, *138*, 47–59.
- Higgins, S., W. S. Broecker, R. Anderson, D. C. McCorkle, and D. Timothy (1999), Enhanced sedimentation along the equator in the western Pacific, *Geophys. Res. Lett.*, *26*, 3489–3492.
- Honjo, S. (1980), Material fluxes and modes of sedimentation in the mesopelagic and bathypelagic zones, *J. Mar. Res.*, *38*, 53–97.
- Honjo, S. (1982), Seasonality and interaction of biogenic and lithogenic particulate flux at the Panama Basin, *Science*, *218*, 883–884.
- Honjo, S., J. Dymond, R. Collier, and S. J. Manganini (1995), Export production of particles to the interior of the equatorial Pacific Ocean during the 1992 EqPac experiment, *Deep Sea Res.*, *42*(2-3), 831–870.
- Klitgord, K. D., and J. D. Mudie (1974), The Galapagos Spreading Centre: A near-bottom geophysical survey, *Geophys. J. R. Astron. Soc.*, *38*, 563–586.
- Knappenberger, M. (2000), Sedimentation rates and Pacific plate motion calculated using seismic cross sections of the Neogene equatorial sediment bulge, M.S. thesis, Boise St. Univ., Boise, Idaho.
- Le Bouteiller, A., A. Leynaert, M. R. Landry, R. Le Borgne, J. Neveux, M. Rodier, J. Blanchot, and S. L. Brown (2003), Primary production, new production, and growth rate in the equatorial Pacific: Changes from mesotrophic to oligotrophic regime, *J. Geophys. Res.*, *108*(C12), 8141, doi:10.1029/2001JC000914.
- Lister, C. R. B. (1976), Control of pelagic sediment distribution by internal waves of tidal period: Possible interpretation of data from the Southern East Pacific Rise, *Mar. Geol.*, *20*, 297–313.
- Lonsdale, P. (1977a), Inflow of bottom water to the Panama Basin, *Deep Sea Res.*, *24*, 1065–1101.
- Lonsdale, P. (1977b), Deep-tow observations at the mounds abyssal hydrothermal field, Galapagos Rift, *Earth Planet. Sci. Lett.*, *36*, 92–110.
- Lonsdale, P., and J. B. Southard (1974), Experimental erosion of north Pacific red clay, *Mar. Geol.*, *17*, M51–M60.
- Loubere, P. (1999), A multiproxy reconstruction of biological productivity and oceanography in the eastern equatorial Pacific for the past 30,000 years, *Mar. Micropaleontol.*, *37*, 173–198.
- Loubere, P., M. Fariduddin, and R. W. Murray (2003), Patterns of export production in the eastern equatorial Pacific over the past 130,000 years, *Paleoceanography*, *18*(2), 1028, doi:10.1029/2001PA000658.
- Loubere, P., F. Mekik, R. Francois, and S. Pichat (2004), Export fluxes of calcite in the eastern equatorial Pacific from the Last Glacial Maximum to present, *Paleoceanography*, *19*, PA2018, doi:10.1029/2003PA000986.
- Lyle, M. (1992), Composition maps of surface sediments of the eastern tropical Pacific ocean, *Proc. Ocean Drill. Program Initial Rep.*, *138*, 101–115.
- Lyle, M., D. W. Murray, B. P. Finney, J. Dymond, J. M. Robbins, and K. Brooksforce (1988), The record of late Pleistocene biogenic sedimentation in the eastern tropical Pacific Ocean, *Paleoceanography*, *3*, 39–59.
- Lyle, M., L. Mayer, N. Pisias, T. Hagelburg, K. Dadey, S. Bloomer, and Leg 138 Shipboard Scientific Party (1992), Downhole logging as a paleoceanographic tool on Ocean Drilling Program Leg 138: Interface between high-resolution stratigraphy and regional syntheses, *Paleoceanography*, *7*, 691–700.
- Lyle, M., A. Mix, and N. Pisias (2002a), Patterns of  $\text{CaCO}_3$  deposition in the eastern tropical Pacific Ocean for the last 150 kyr: Evidence for a southeast Pacific depositional spike during marine isotope stage (MIS) 2, *Paleoceanography*, *17*(2), 1013, doi:10.1029/2000PA000538.
- Lyle, M., L. M. Liberty, T. C. Moore Jr., and D. K. Rea (2002b), Development of a seismic stratigraphy for the Paleogene sedimentary section, central equatorial Pacific Ocean, *Proc. Ocean Drill. Program Initial Rep.*, *199*. (Available at [http://www-odp.tamu.edu/publications/199\\_IR/199ir.htm](http://www-odp.tamu.edu/publications/199_IR/199ir.htm))
- Mantyla, A. W. (1975), On the potential temperature in the abyssal Pacific Ocean, *J. Mar. Res.*, *33*, 341–353.
- Marcantonio, F., R. F. Anderson, M. Stute, N. Kumar, P. Schlosser, and A. Mix (1996), Extraterrestrial  $^3\text{He}$  as a tracer of marine sediment transport and accumulation, *Nature*, *383*, 705–707.
- Marcantonio, F., R. F. Anderson, S. Higgins, M. Stute, P. Schlosser, and P. Kubik (2001), Sediment focusing in the central equatorial Pacific Ocean, *Paleoceanography*, *16*, 260–267.
- Mayer, L. A., T. H. Shipley, and E. L. Winterer (1986), Equatorial Pacific seismic reflectors as indicators of global oceanographic events, *Science*, *233*, 761–764.
- Mitchell, N. C. (1995), Characterising the extent of volcanism at the Galapagos Spreading Centre using Deep Tow sediment profiler records, *Earth Planet. Sci. Lett.*, *134*, 459–472.
- Mitchell, N. C. (1996), Creep in pelagic sediments and potential for morphologic dating of marine fault scarps, *Geophys. Res. Lett.*, *23*, 483–486.
- Mitchell, N. C. (1998), Sediment accumulation rates from Deep Tow profiler records and DSDP Leg 70 cores over the Galapagos Spreading Centre, in *Geological Evolution of Ocean Basins: Results From the Ocean Drilling Program, Spec. Pap.*, vol. 131, edited by A. Cramp et al., pp. 199–209, Geol. Soc., London.
- Mitchell, N. C., and M. Lyle (2005), Patchy deposits of Cenozoic pelagic sediments in the central Pacific, *Geology*, in press.
- Mitchell, N. C., M. W. Lyle, M. B. Knappenberger, and L. M. Liberty (2003), Lower Miocene to present stratigraphy of the equatorial Pacific sediment bulge and carbonate dissolution anomalies, *Paleoceanography*, *18*(2), 1038, doi:10.1029/2002PA000828.
- Mix, A., R. Tiedemann, P. Blum, and the Shipboard Scientific Party (2003), *Proceedings of the Ocean Drilling Program, Initial Reports*, vol. 202, Ocean Drill. Project, College Station, Tex. (Available at [http://www-odp.tamu.edu/publications/202\\_IR/202ir.htm](http://www-odp.tamu.edu/publications/202_IR/202ir.htm))
- Moore, W. S., K. Teh-Lung, J. D. Macdougall, V. M. Burns, R. Burns, J. Dymond, M. W. Lyle, and D. Z. Piper (1981), Fluxes of metals to a manganese nodule: Radiochemical, chemical, structural, and mineralogical studies, *Earth Planet. Sci. Lett.*, *52*, 151–171.
- Murray, R. W., M. Leinen, and A. R. Isern (1993), Biogenic flux of Al to sediment in the central equatorial Pacific Ocean: Evidence for increased productivity during glacial periods, *Paleoceanography*, *8*(5), 651–671.
- Murray, R. W., C. Knowlton, M. Leinen, A. Mix, and C. H. Polsky (2000), Export production and carbonate dissolution in the central equatorial Pacific Ocean over the past 1 Myr., *Paleoceanography*, *15*(6), 570–592.
- Ninkovich, D., and N. J. Shackleton (1975), Distribution, stratigraphic position and age of ash layer “L” in the Panama Basin region, *Earth Planet. Sci. Lett.*, *27*, 20–34.
- Normark, W. R., and F. N. Spiess (1976), Erosion on the Line Islands archipelagic apron: Effect of small-scale topographic relief, *Geol. Soc. Am. Bull.*, *87*, 286–296.

- Pak, H., and J. R. V. Zaneveld (1973), The Cromwell Current on the east side of the Galapagos Islands, *J. Geophys. Res.*, **78**, 7845–7859.
- Paytan, A., M. Kastner, and F. Chavez (1996), Glacial to interglacial fluctuations in productivity in the equatorial Pacific as indicated by marine barite, *Science*, **214**, 1355–1357.
- Paytan, A., M. Lyle, A. Mix, and Z. Chase (2004), Climatically driven changes in oceanic processes throughout the equatorial Pacific, *Paleoceanography*, **19**, PA4017, doi:10.1029/2004PA001024.
- Pedersen, T. F. (1983), Increased productivity in the eastern equatorial Pacific during the Last Glacial Maximum (19,000 to 14,000 yr B.P.), *Geology*, **11**, 16–19.
- Pedersen, T. F., M. Pickering, J. S. Vogel, J. N. Southon, and D. E. Nelson (1988), The response of benthic foraminifera to productivity cycles in the eastern equatorial Pacific: Faunal and geochemical constraints on glacial bottom water oxygen levels, *Paleoceanography*, **3**, 157–168.
- Pedersen, T. F., B. Nielsen, and M. Pickering (1991), The timing of late Quaternary productivity pulses in the Panama Basin and implications for atmospheric CO<sub>2</sub>, *Paleoceanography*, **6**, 657–679.
- Schott, F. A., R. Zantopp, L. Stramma, M. Dengler, J. Fischer, and M. Wibaux (2004), Circulation and deep-water export at the western exit of the subpolar north Atlantic, *J. Phys. Oceanogr.*, **34**, 817–843.
- Somayajulu, B. L. K., G. R. Heath, T. C. Moore Jr., and D. S. Cronan (1971), Rates of accumulation of manganese nodules and associated sediment from the equatorial Pacific, *Geochim. Cosmochim. Acta*, **35**, 621–624.
- Taft, B. A., S. R. Ramp, J. G. Dworski, and G. Holloway (1981), Measurements of deep currents in the central North Pacific, *J. Geophys. Res.*, **86**, 1955–1968.
- Thomas, E., K. K. Turekian, and K.-Y. Wei (2000), Productivity control of fine particle transport to equatorial Pacific sediment, *Global Biogeochem. Cycles*, **14**, 945–955.
- van Andel, T. H., and R. D. Ballard (1979), The Galapagos Rift at 86°W: 2. Volcanism, structure, and evolution of the rift valley, *J. Geophys. Res.*, **84**, 5390–5406.
- Watkins, N. D., and J. P. Kennett (1971), Erosion of deep-sea sediments in the Southern Ocean between longitudes 70°E and 190°E and contrasts in manganese nodule development, *Mar. Geol.*, **23**, 103–111.
- Wyrtki, K., and B. Kilonsky (1984), Mean water and current structure during the Hawaii-to-Tahiti shuttle experiment, *J. Phys. Oceanogr.*, **14**, 242–254.
- Yu, E.-F., R. Francois, M. P. Bacon, S. Honjo, A. P. Fleer, S. J. Manganini, M. M. Rutgers van der Loeff, and V. Ittekkot (2001a), Trapping efficiency of bottom-tethered sediment traps estimated from the intercepted fluxes of <sup>230</sup>Th and <sup>231</sup>Pa, *Deep Sea Res.*, **48**, 865–889.
- Yu, E.-F., R. Francois, M. P. Bacon, and A. P. Fleer (2001b), Fluxes of <sup>230</sup>Th and <sup>231</sup>Pa to the deep sea: Implications for the interpretation of excess <sup>230</sup>Th and <sup>231</sup>Pa/<sup>230</sup>Th profiles in sediments, *Earth Planet. Sci. Lett.*, **191**, 219–230.

---

M. Lyle, Center for Geophysical Investigation of the Shallow Subsurface, Boise State University, MS 1536, 1910 University Drive, Boise, ID 83725, USA. (mlyle@cgiss.boisestate.edu)

J. I. Martinez, Departamento de Geología, Universidad EAFIT, A.A. 3300 Medellín, Colombia.

N. Mitchell, School of Earth, Ocean and Planetary Sciences, Cardiff University, P. O. Box 914, Cardiff CF10 3YE, UK.

A. Mix and N. Pisis, College of Ocean and Atmospheric Sciences, Oregon State University, Corvallis, OR 97331, USA.

A. Paytan, Department of Geological and Environmental Sciences, Stanford University, Stanford, CA 94305-2115, USA.

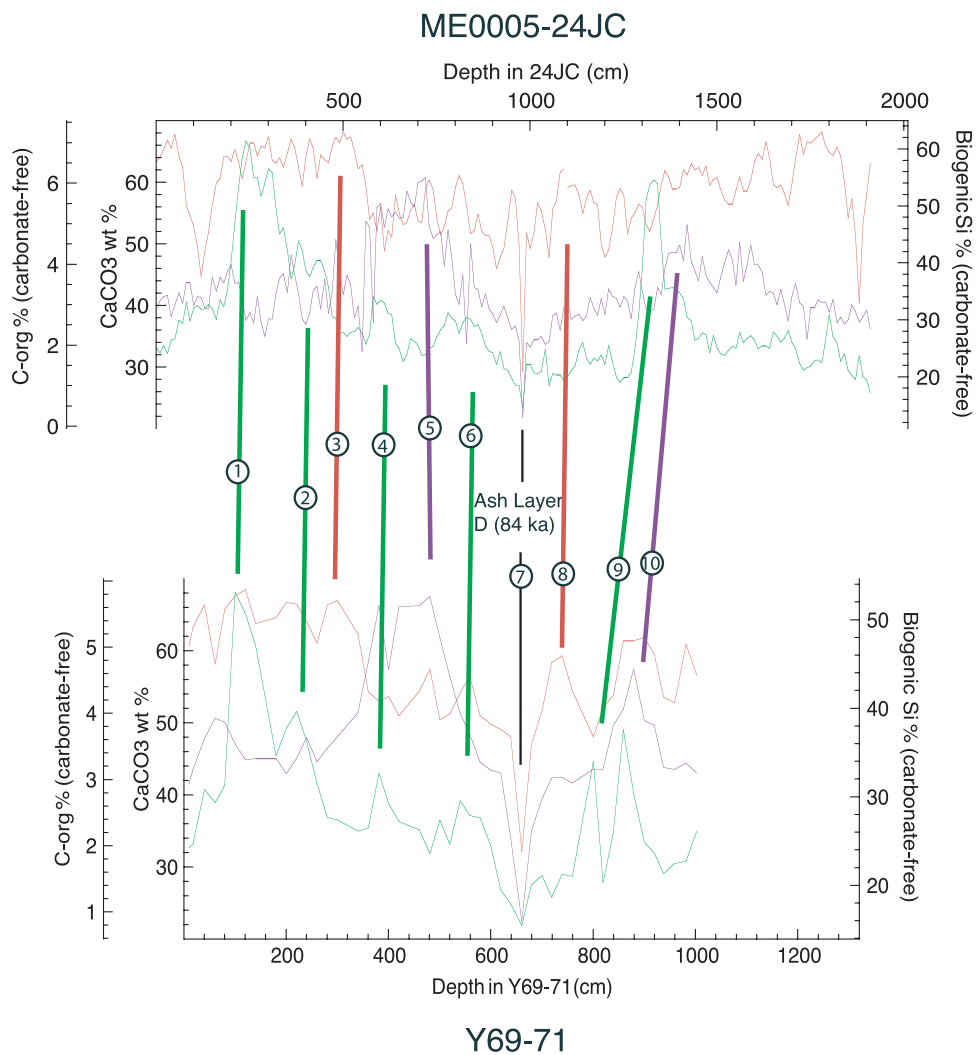


**Figure 2.** A comparison of  $\text{CaCO}_3$  (red), carbonate-free biogenic silica (purple), and carbonate-free  $\text{C}_{\text{org}}$  wt % (green) depth series between Y69-71 and ME0005-24JC. The cores have been lined up, and depths in each core are linearly scaled to each other based on ash layer D (84 ka; *Drexler et al.* [1980]). Lines mark correlations between the three records in each core, and numbers mark events in Figure 3. For at least the last 100 kyr, common sediment events between the two cores line up, indicating no change in relative sedimentation rate.

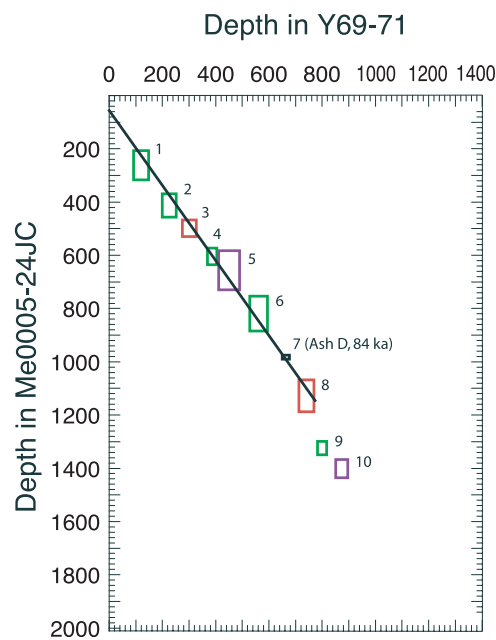
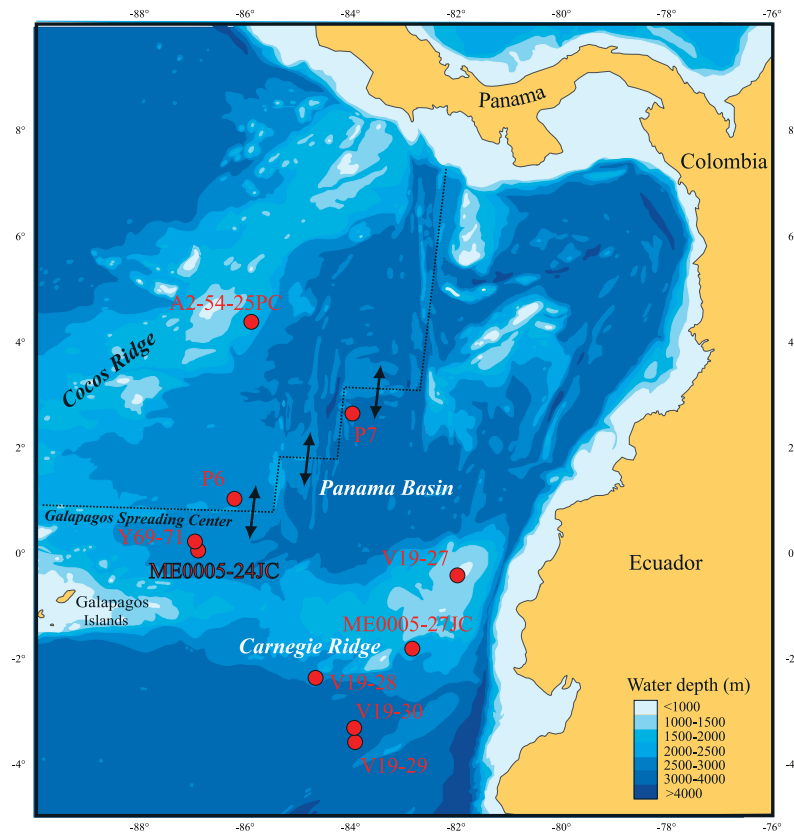


**Figure 3.** A Shaw plot to estimate relative sedimentation rates between Y69-71 and ME0005-24JC, showing that the relative sedimentation rate between the two cores has remained constant for the last 100 kyr. Each event shown in Figure 2 is represented by boxes here; red represents a  $CaCO_3$  event, purple represents biogenic silica, and green represents  $C_{org}$ . Numbers of the events are the same as in Figure 2.



Scale: 1:9375375 at Latitude 0°

**Figure 4.** A map of the Panama Basin and northern Peru Basin showing where the Last Glacial Maximum sedimentation event has been found [Lyle *et al.*, 2002a; Pedersen *et al.*, 1988; Lyle *et al.*, 1988; Pedersen, 1983; M. Lyle and J. Guarín-Tirado, unpublished data, 2001]. This event is not confined to a small area. Instead, it has been found over a 6° square of the Panama Basin and northern Peru Basin east of the Galapagos. If this event were to be caused by sediment focusing, much of the rest of the eastern tropical Pacific must have been stripped of sediment during the Last Glacial Maximum. There is insufficient area on ridges to provide sediment for focusing.